CHAPTER TWO

Synthesis and Characterization of Catalysts

2.1 PREPARATION OF CATALYST

A series of chromium(III), iron(III) and chromium-iron mixed-metal complexes were synthesized using method discovered by Gan, S.N. *et al.* Common chromium(III) and iron(III) salts react with carboxylic acid to produce tri-oxo-nuclear complexes (Beatrice, 2009; Gan *et al.*, 2000; Gan *et al.*, 1987; Ooi, 1996; Tan, 2007; Wong, 2010). **Table 2.1** shows the combination of metals and ligands for the preparation of the complexes and the recommended molecular formulae of the complexes. The complexes will be used in the polymerization of ethylene as catalysts for the next stage.

Table 2.1: Synthesis of complexes

Complex	Metal	Ligand	Molecular formula
CI[1]	Cr	CH_3COOH	$[Cr_3O(CH_3CO_2)_6.3H_2O]NO_3CH_3CO_2H$
CI[2]	Cr, Fe (2:1)	CH_3COOH	$[Cr_2FeO(CH_3CO_2)_6.3H_2O]NO_3CH_3CO_2H$
CI[3]	Cr, Fe (1:2)	CH_3COOH	$[CrFe_2O(CH_3CO_2)_6.3H_2O]NO_3CH_3CO_2H$
CI[4]	Fe	CH_3COOH	$[Fe_3O(CH_3CO_2)_6.3H_2O]NO_3CH_3CO_2H$
CI[5]	Cr	C_6H_5COOH	$[Cr_3O(C_6H_5CO_2)_6.3H_2O]NO_3C_6H_5CO_2H$

2.1.1 Synthesis of chromium(III) acetate, CI[1]

Glacial acetic acid (CH_3COOH) was first purified by distillation while chromium(III) nitrate nonahydrate ($Cr(NO_3)_3.9H_2O$) was ground to a fine powder. After that, chromium salt (10.00 g) and acetic acid (24.0 ml) were mixed into a 250 ml round bottom flask and then refluxed for 10 hours. Silica gel was used as drying agent to avoid the formation of moisture in the refluxing system. The hot-dark-green solution formed was filtered into a flask and left to cool slowly to room temperature while fine powdery solid began to form. The products were collected by filtration, washed repeatedly with chloroform and dried in a vacuum oven for 24 hours at 60^{o}C. A shiny, dark green crystalline solid (**Figure 2.1**) was produced with a yield of 70.4%.

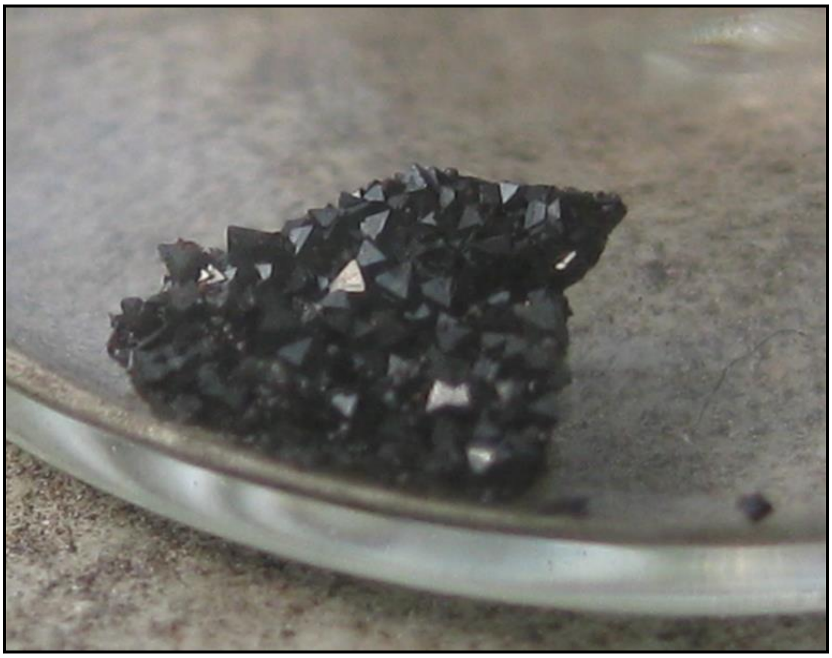

Figure 2.1: Crystal of **CI[1]** complex

2.1.2 Synthesis of mixed-metal (Cr-Fe) acetate, CI[2] and CI[3]

Iron(III) nitrate nonahydrate ($Fe(NO_3)_3.9H_2O$) and chromium(III) nitrate nonahydrate ($Cr(NO_3)_3.9H_2O$) were added into glacial acetic acid (29.1 ml). The ratio of Cr/Fe was 2:1 **(**$Cr(NO_3)_3.9H_2O$ = 8.04 g; $Cr(NO_3)_3.9H_2O$ = 4.01 g) for **CI[2]** and 1:2 **(**$Cr(NO_3)_3.9H_2O$ = 4.03 g; $Cr(NO_3)_3.9H_2O$ = 8.08 g) for **CI[3]**. The mixture was refluxed for 10 hours and the resulting solution was cooled to room temperature after filteration. The crystalline products were collected, washed thoroughly with chloroform and dried for 24 hours in vacuum oven at 60^oC.

2.1.3 Synthesis of iron(III) acetate, CI[4]

Iron(III) nitrate nonahydrate ($Fe(NO_3)_3.9H_2O$) (10.00 g) was added to glacial acetic (24.0 ml) acid in a 250 ml round bottom flask. The mixture was refluxed for 10 hours and the resulting red-hot-solution was filtered into a flask then left to cool to room temperature. The products were collected, washed with chloroform and left to dry for 24 hours in vacuum oven at 60^oC.

2.1.4 Synthesis of chromium(III) benzoate, CI[5]

Benzoic acid (C_6H_5COOH) (20.75 g) was first ground to form a fine powder was mixed with chromium(III) nitrate nonahydrate ($Cr(NO_3)_3.9H_2O$) (4.00 g) into a 250 ml round bottom flask before refluxing for 10 hours. The green solution was filtered into a flask before left to cool to form a green powder. After filtering and washing repeatedly with chloroform, the products were dried in a vacuum oven for 24 hours at 60^oC. A green powder with a yield of 87.1% was produced.

2.2 CHARACTERIZATIONS OF COMPLEXES

The complexes were characterized by IR spectroscopy, UV-visible spectroscopy, CHN-elemental analysis, inductively coupled plasma optical emission spectrometry (ICP-OES), thermal gravimetric analysis (TGA), and X-ray crystallography. Some physical properties such as solubility and appearance of the complexes have also been recorded.

2.2.1 Solubility test

The solubility test was carried out using common methods. 0.1 g of complex was dissolved in 10.0 ml of solvent. The mixture was shaken vigorously for a several time.

2.2.2 IR spectroscopy

IR spectrometer model RX-1 Perkin Elmer was used to record spectra in the range of 4000 – 400 cm^{-1} for complexes. The complexes were mixed with dried KBr and ground to become a well-mixed powder. The mixture was then pressed into a disc before analysing by IR spectrometer.

2.2.3 UV-visible spectroscopy

The reflectance container was filled up with samples before being set up to the UV-instrument. The spectra were obtained from the reflectance electronic technique by using UV-3600 Shimadzu UV-Vis-NIR Spectrophotometer. Complexes were scanned from 200 – 1000 nm.

2.2.4 Metal content analysis

Samples were dissolved in water to a known concentration in a volumetric flask. The metal-contain analysis was carried out by using Perkin-Elmer Optima 5400 ICP-OES and XRF spectrometer model µEDX-1200/1300/1400 Shimadzu to measure the percentage of metal and to confirm the ratio of chromium and iron metal in the complexes.

2.2.5 CHN-elemental Analysis

Carbon, hydrogen and nitrogen elements were analysed by series II CHNS/O analyser 2400 Perkin Elmer. The preparation of sample for analysis was carried out by weighing about 0.02 g into aluminium pan. The aluminium pan was folded before analysed by CHN-analyser instrument.

2.2.6 Thermal gravimetric analysis (TGA)

A sample about 10 mg of the complexes was transferred into TGA pan and analysed using model Pyris Diamond TG/DTA of Perkin Elmer with a scan rate of 20°C/min. The measurement was performed under nitrogen atmosphere with a flow rate of 20 ml/min and temperature ranging from 50 – 900°C.

2.2.7 X-ray Crystallography

Data collected for single crystal X-ray diffraction were performed on a Bruker SMART APEX diffractometer operating with graphite-monochromator Mo Kα radiation ($\lambda = 0.71073$ Å) at 100 K. The intensities were collected using the ω -2θ scan mode, in the range $2.0^{o} < \theta < 27.5^{o}$. All structures were solved by direct method by using SHELXS-97 and refined by full matrix least-square methods on F^2 with the use of the SHELXL-97 program package (semi-empirical absorption corrections were applied using SADABS program).

2.3 RESULTS AND DISCUSSION

2.3.1 Physical properties

The preparation of **CI[1]** was carried out using different conditions by varying chromium salts/acetic acid molar ratio, refluxing time and different method for cooling the product solution. **Table 2.2** shows the highest yield of complex was obtained by using a molar ratio of chromium salts/acetic acid of 1:17 and refluxing time of 10 hours. Preparation of complex using molar ratio of chromium salts/acetic acid lower than 1:10 results in lower yields (Ooi, 1996; Tan, 2007). The product yield can be enlarged by cooling the product solution in refrigerator at 0 – 2^{o}C for several days. However, the yield was found to decrease as the reaction time and the molar ratio of chromium salts/acetic acid were increased.

Table 2.2: Synthetic parameter and parameters of the synthesized complexes

Complex	Cr/Fe ratio	Metal/CH_3COOH ratio	Reaction time (hours)	Yield (%)	Complex colour	Soluble	Insoluble
CI[1]	3:0	1:6	10	31.2	Green solid	Methanol, ethanol, water	Toluene, chloroform
CI[1]	3:0	1:10	6	55.4	Green solid	Methanol, ethanol, water	Toluene, chloroform
CI[1]	3:0	1:10	10	55.7	Green solid	Methanol, ethanol, water	Toluene, chloroform
CI[1]	3:0	1:17	10	70.3	Green solid	Methanol, ethanol, water	Toluene, chloroform
CI[1]	3:0	1:17*	10	79.2	Green solid	Methanol, ethanol, water	Toluene, chloroform
CI[1]	3:0	1:17	24	55.2	Green solid	Methanol, ethanol, water	Toluene, chloroform
CI[1]	3:0	1:21	24	65.2	Green solid	Methanol, ethanol, water	Toluene, chloroform
CI[2]	2:1	1:17	10	71.1	Dark purple	Methanol, ethanol, water	Toluene, chloroform
CI[3]	1:2	1:17	10	70.9	Reddish-purple	Methanol, ethanol, water	Toluene, chloroform
CI[4]	0:3	1:17	10	73.1	Red solid	Methanol, ethanol, water.	Toluene, chloroform
CI[5]	3:0	1:17**	10	87.1	Green solid	Methanol, ethanol, water	Toluene, chloroform

1:17* = cooled in refrigerator **benzoic acid was used

Table 2.2 shows yields of the synthesized of chromim(III), iron(III), mixed-metal (Cr-Fe) acetate and the yield of complexes. **CI[4]** was prepared by heating Fe(III) salt with acetic acid in molar ratio 1:17 for 10 hours to give 73.1% product yield. Meanwhile, under the same condition the yield of **CI[2]** and **CI[3]** obtained were 71.1% and 70.9% respectively. Using a different metal ratio and metal-acetic acid ratio, Cr(III) complex was synthesized using benzoic acid as ligand to replace acetic acid (**CI[5]**). The yield of **CI[5]** was 87.1%. Therefore, five different complexes were prepared in this study.

The physical appearance and the solubility properties of the complexes are recorded in **Table 2.2**. All complexes are soluble in alcohol and water but insoluble in toluene and chloroform. Meanwhile, the colours of complexes change as different molar ratios of chromium/iron were used in the preparation of the complex. When the Cr/Fe ratio is 2:1 the complex colour is dark purple, while when the Cr/Fe ratio is 1:2, a reddish-purple complex is obtained. The colour of the complexes are shown in **Table 2.2**.

2.3.2 UV-visible

The complexes have been reported to form an oxo-centred trinuclear carboxylate where three metal ions were bridged by a μ_3-oxo atom at the centre, forming a triangular arrangement (refer to **Figure 1.1**). Each pair of the three metal ions was bridged by two acetate ligands. The trigonally coordinated oxygen atom in the centre of the triangle and the terminal water molecules will form an approximately octahedral coordination at each metal ion. UV-visible reflectance spectra of the complexes are summarized in **Table 2.3**. Interpretation of the spectra was explained based on literature study (Baranwal & Fatma, 2005; Baranwal, *et al.*, 2009; Dubicki & Day, 1972; Fernandes, *et al.*, 1996; Lawrence, *et al.* 2012 ; Lawrence, *et al.*, 2011; Losada, *et al.*, 1997; Schatschneider & Perumareddi, 2005; Yazdanbakhsh, *et al.*, 2009; Yazdanbakhsh, *et al.*, 2010).

Table 2.3: UV-visible reflectance spectra of the complexes

Complex	Absorption, λ (nm)
CI[1]	257, 440, 588, 670(sh), 714, 822, 994
CI[2]	345, 360, 445, 512, 648, 698, 720, 840, 984
CI[3]	279, 341, 443, 525(sh), 648, 702, 725(sh), 966
CI[4]	204, 319, 335, 415(sh), 475(sh), 540(sh), 969
CI[5]	223, 281, 450, 588, 670(sh)

The electronic spectra of oxo-centred trinuclear complexes can be interpreted with good approximation in the terms of d-d transitions of individual metal ions, together with the ligands-metal charge transfer transitions. The visible spectra of pseudo-octahedral Cr(III) complexes are expected to display two dominant d-d bands, corresponding to the spin-allowed $^4A_{2g}\rightarrow{}^4T_{2g}$ and $^4A_{2g}\rightarrow{}^4T_{1g}$ transitions. **Figure 2.2a** shows electronic spectra for **CI[1]** with three broad absorption at 257 nm, 440 nm and 588 nm. A broad band at 257 nm indicates $\pi\rightarrow\pi^*$ double bond in acetate ligand while the other two broad bands at 588 nm and 440 nm are corresponding to $^4A_{2g}\rightarrow{}^4T_{2g}$ and $^4A_{2g}\rightarrow{}^4T_{1g}$ transitions respectively. At 670 nm, the shoulder band can be assigned as a low-symmetry component of $^4T_{2g}$ (Bond *et al.*, 1998; Dubicki & Day, 1972; Yazdanbakhsh, *et al.*, 2009).

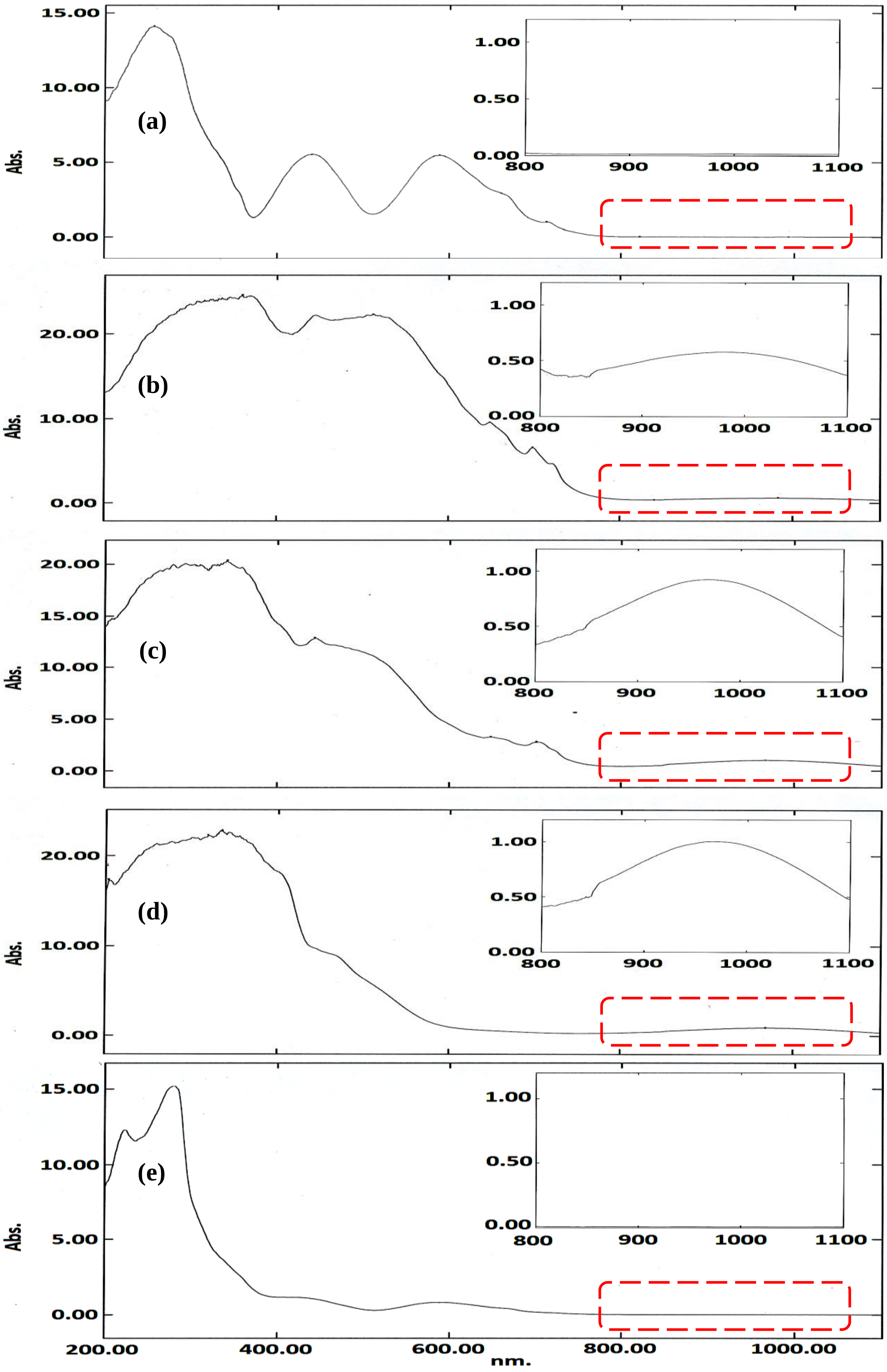

Figure 2.2: The electronic spectrum of complexes; (a) complex **CI[1]** (b) complex **CI[2]** (c) complex **CI[3]** (d) complex **CI[4]** (e) complex **CI[5]**

Structure of **CI[2]** and **CI[3]** have numerous similarities and the only difference in these complexes is the metal ions. There are two Cr(III), one Fe(III) in $[Cr_2FeO(CH_3CO_2)_6(H_2O)_3]^+$ cation cluster and one Cr(III), two Fe(III) in $[CrFe_2O(CH_3CO_2)_6(H_2O)_3]^+$ cation cluster. **Figures 2.2b** and **2.2c** show the electronic transitions of these complexes and the absorption peaks are recorded in **Table 2.3**. The shoulder observed at ~370 nm is tentatively assigned to Fe(III) but one expects it to be influenced by a combination of the charge transfer band of the Cr(III) and Fe(III). The bands at 445 nm of **CI[2]** and 443 nm of **CI[3]** can be assigned to $^4A_{2g}\rightarrow{}^4T_{1g}$ of Cr(III), while the broad band with a centre at 512 nm of **CI[2]** and a shoulder at 525 nm are assigned to the $^4A_{2g}\rightarrow{}^4T_{2g}$ of Cr(III) and the much weaker $^6A_{1g}\rightarrow(^4A_{1g}, {}^4E_g)$ of Fe(III). The transition occurring at 648 nm is assigned to $^6A_{1g}\rightarrow{}^4T_{2g}$ (^4G) of Fe(III). The remaining transitions are primarily assigned to the low-symmetry component of the $^4T_{2g}$ of Cr(III) and the weak peaks at 984 nm of **CI[2]** and 966 nm of **CI[3]** are assigned to the $^6A_{1g}\rightarrow{}^4T_{1g}$ (^4G) of Fe(III) in a pseudo-octahedral environment (Lawrence, *et al.* 2012).

Tri-iron system is not spectroscopically well understood at present. The electronic spectrum (**Figure 2.2d**) appears broad and largely featureless with intense charge transfer character from 500 nm downwards because the strong ligand-metal charge transfer transition partially obscures other bands. The only low-intensity transition observed at 969 nm is refered to the $^6A_{1g}\rightarrow{}^4T_{1g}$ (^4G) of Fe(III) in a pseudo-octahedral environment (Lawrence, *et al.* 2012; Lawrence, *et al.*, 2011; Losada, *et al.*, 1997)

CI[5] which holds six benzoate ligands and as **CI[1]**, it has a pseudo-octahedral environment with tri-chromium metal-based. The UV-visible spectrum in **Figure 2.2e** shows two strong bands at 223 nm and 281 nm assigned to $n\rightarrow\pi^*$ and $\pi\rightarrow\pi^*$ electronic transition of the aromatic ligands respectively. The ${}^4A_{2g}\rightarrow{}^4T_{1g}$ and ${}^4A_{2g}\rightarrow{}^4T_{2g}$ transitions can be observed at 425 nm and 588 nm.

2.3.3 IR spectroscopy

Two characteristic bands of free acetate ion are mostly present at 1560 cm^{-1} and 1416 cm^{-1} and the difference in frequency is 140 cm^{-1}. These bands are sensitive to the modes of coordination of the acetate group to metal ions. In unidentate complex, the separation is much larger than 200 cm^{-1} because ν(C=O) is higher than ν_{asym}(OCO) while ν(C−O) is lower than ν_{sym}(OCO). In bridging mode, the separation of ν_{asym}(OCO) and ν_{sym}(OCO) are in the range of 100 – 200 cm^{-1} (Gan, *et al.*, 1987). Free carboxylic acids usually give two characteristic bands ν(C=O) and δ (O−H) at 1710 cm^{-1} and 935 cm^{-1} respectively. The IR spectra of complexes in this study are similar to that reported in the literature (Baranwal, *et al.* 2002; Baranwal & Fatma, 2005; Baranwal, *et al.*, 2009; Fernandes, *et al.*, 1996; Gan, *et al.*, 1987; Glowiak, *et al.*, 1996; Losada, *et al.*, 1997; Nakamoto, *et al.*, 1997; Wu, *et al.*, 1998; Yazdanbakhsh, *et al.*, 2009; Yazdanbakhsh, *et al.*, 2010)

Table 2.4: Selected IR spectra bands of complexes

Band assignment	**Group frequency, wavenumber (cm^{-1})**				
	CI[1]	**CI[2]**	**CI[3]**	**CI[4]**	**CI[5]**
ν_{asym}(OCO)	1610	1603	1599	1592	1574
ν_{sym}(OCO)	1455	1453	1445	1449	1421
ν_{asym}(NO_3^-)	1385	1385	1385	1385	1385
ν_{sym}(NO_3^-)	1039	1043	1037	1036	1026
ν(M−H_2O)	-	-	-	-	708
δ(OCO)	663	672	667	662	668
π(OCO)	623	623	619	614	-
ν_{asym}(M_3−O)	-	-	-	527	524
ν(Cr−O)	439, 408	420, 410	424, 409	-	-

IR spectral data of the complexes are given in **Table 2.4**. The characteristic C=O stretching of the free carboxylic acid band is found absent in all complexes. A weak band of O−H deformation of the free carboxylic acid band can be observed at 930 – 960 cm^{-1} indicating the presence of solvated carboxylic acids (**Figures 2.3**). The complexes exhibit a medium to strong band at 3448 – 3337 cm^{-1} indicating the O−H stretching vibration of the free hydroxyl group of the hydroxycarboxylic acid solvated and coordinated by water molecules.

Two bands of ν_{asym}(OCO) and ν_{sym}(OCO) vibrations of the carboxylate ions can be observed in the range of 1590 – 1610 cm^{-1} and 1445 – 1455 cm^{-1} respectively. **Table 2.5** shows the differences between the symmetric and antisymmetric stretches, $\Delta[\nu_{asym}$(OCO) - ν_{sym}(OCO)] giving 155 cm^{-1}, 158 cm^{-1}, 154 cm^{-1}, 143 cm^{-1} and 153 cm^{-1} for **CI[1]**, **CI[2]**, **CI[3]**, **CI[4]** and **CI[5]** respectively. Therefore, all the carboxylate groups of carboxylic acids are bound to the metals in bidentate and bridging mode involving coordination of both the oxygen atoms of the ligands. Two medium bands observed at 660 – 680 cm^{-1} could be assigned to $\delta(CO_2)$ while at 610 – 625 cm^{-1} is attributed to $\pi(CO_2)$ of the bridging carboxylate anion.

Table 2.5: The differences between ν_{asym}(OCO) and ν_{sym}(OCO) of complexes

Complex	ν_{asym}(OCO) / cm^{-1}	ν_{sym}(OCO) / cm^{-1}	$\Delta\nu$(OCO) / cm^{-1}
CI[1]	1610	1455	155
CI[2]	1603	1453	158
CI[3]	1599	1445	154
CI[4]	1592	1449	143
CI[5]	1574	1421	153

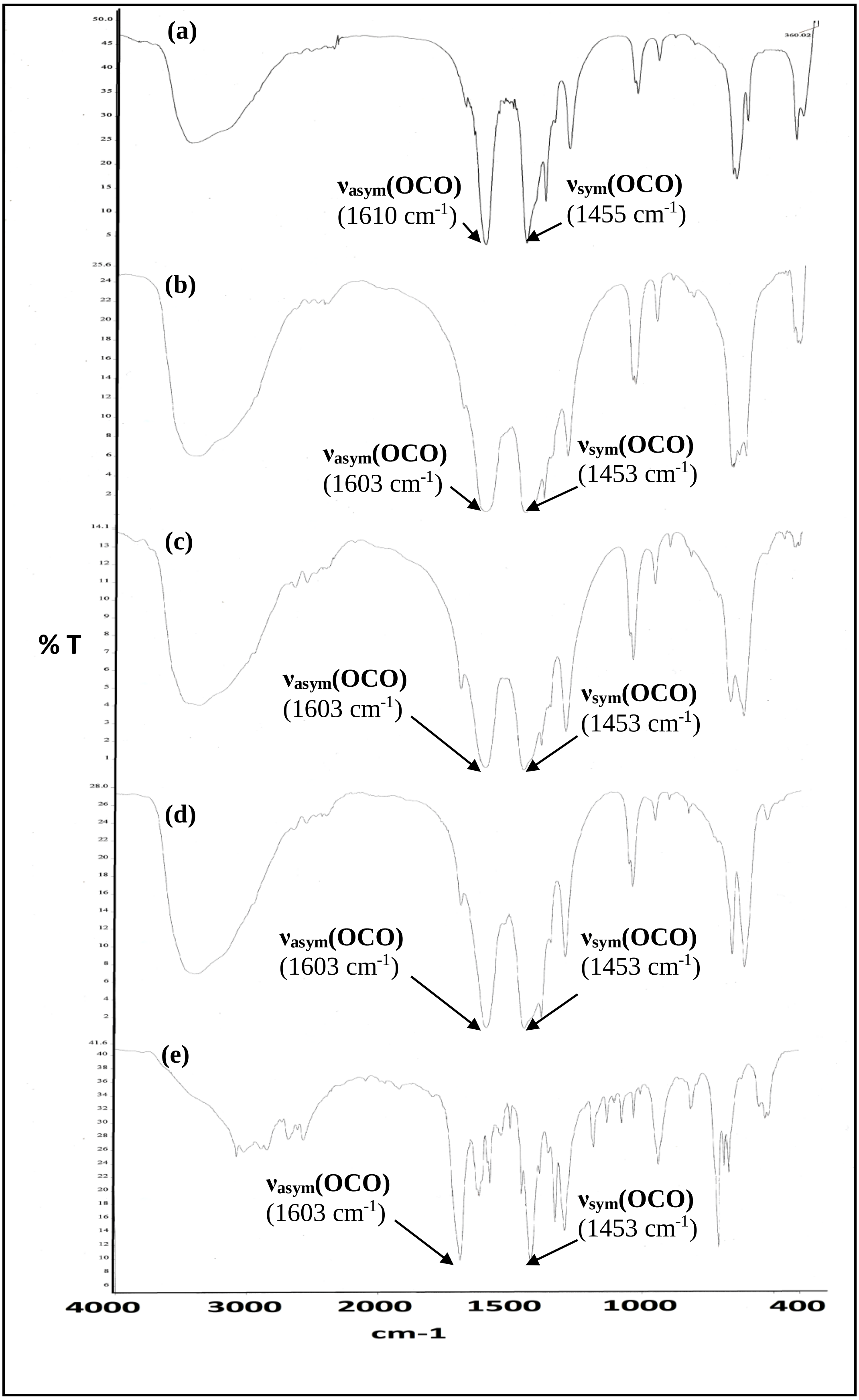

Figure 2.3: IR spectra of complexes: (a) Complex **CI[1]**, (b) Complex **CI[2]**, (c) Complex **CI[3]**, (d) Complex **CI[4]**, (e) Complex **CI[5]**

The presence of NO_3^- can also be assigned in the IR spectrum where the band can be found at 1385 cm^{-1} due to $\nu_{asym}(NO_3^-)$. Yazdanbakhsh, *et al.* (2009) reported that these spectra follow through the appearance of the $\nu_3(E)$ [$\nu_d(NO)$] mode of the D_3h ionic nitrate. Besides that, some researchers reported that $\nu_{sym}(NO_3^-)$ bands appear at 1036 – 1043 cm^{-1} (Fernandes, *et al.*, 1996).

There are three metal ions which bond with O at the centre to form an oxo-centred trinuclear complex. Most of the researchers agreed that the band for asymmetric vibration of metals, $\nu_{asym}(M_3O)$ will appear at 540 – 520 cm^{-1} but in a form of weak band (Asamaki *et al.*, 1995; Nakamoto, *et al.*, 1999; Wu, *et al.*, 2000). Two weak bands are observed in region of ~430 cm^{-1} and 410 cm^{-1} which point to the coordination of carboxylate oxygen to each Cr ion in the trinuclear cage yielding the Cr−O vibration modes (Glowiak, *et al.*, 1996). It is worth to mention that the band corresponding to $\nu(M{-}H_2O)$ at ~705 cm^{-1} is missing in all IR spectra of the complexes except in **CI[5]** which was observed at 708 cm^{-1}.

The existence of aromatic ring in **CI[5]** complex gives a significant difference in the IR spectrum. The presence of aromatic ring can be verified based on the C−H and C=C−C ring-related vibrations. Coates, J. reported that the C−H stretching is exhibited as a multiplicity of weak-to-moderate bands observed above 3000 cm^{-1} while the C=C−C aromatic ring stretching usually appears as a pair of band structure with some splitting around 1600 and 1500 cm^{-1}. In this case, $\nu(C{=}C)$ aromatic is observed at 1689 cm^{-1}, 1617 cm^{-1} and 1495 cm^{-1} which in agreement with results from earlier work. There are several bands observed at 1225 – 950 cm^{-1} and 900 – 670 cm^{-1} indicating aromatic C−H in-plane bend and out-of-plane bend respectively (Borawska, *et al.*, 2009; Coates, 2000).

2.3.4 Elemental analysis

The complexes contain several elements which are metal, carbon, hydrogen, nitrogen and oxygen. **Table 2.6** presents the compositions of the elements in the complexes. The percentages of elements which show an agreement between theoretical and experimental values prove that the complexes were successfully prepared as proposed. Moreover, the compositions of Cr and Fe metals in **Tables 2.6** and **2.7** can be used to calculate the ratio of Cr/Fe. Based on ICP-OES analysis, the ratio of Cr/Fe in **CI[2]** is 2.04:1 and in **CI[3]** is 1:2.14. Meanwhile, the ratio of Cr/Fe obtained from XRF analysis for **CI[2]** and **CI[3]** were 2.19:1 and 1:2.27 respectively.

Table 2.6: Compositions of elemental in complexes

Complex	**Theoretical (%)**					**Experimental (%)**				
	Cr	**Fe**	**C**	**H**	**N**	**Cr**	**Fe**	**C**	**H**	**N**
CI[1]	22.2	-	23.9	4.0	2.0	22.9	-	24.4	4.2	2.4
CI[2]	14.7	7.9	23.8	4.0	2.0	15.1	7.7	23.5	4.3	2.3
CI[3]	7.3	15.8	23.7	4.0	2.0	7.4	15.9	24.1	4.6	2.5
CI[4]	-	23.5	23.5	3.9	2.0	-	23.7	24.0	4.0	2.2
CI[5]	13.7	-	44.4	3.7	1.2	13.3	-	44.9	3.7	1.1

*metal content (Cr and Fe) were determine by ICP-OES

Table 2.7: Percentage of Cr metal and Fe metal analysed by XRF analysis

Complex	Theoretical (%)		Experimental (%)	
	Chromium	Iron	Chromium	Iron
CI[1]	100.0	0.0	100.0	0.0
CI[2]	66.7	33.3	68.4	31.2
CI[3]	33.3	66.7	30.6	69.4
CI[4]	0.0	100.0	0.1	99.9
CI[5]	100.0	0.0	98.7	0.4

2.3.5 Thermal gravimetric analysis (TGA)

Thermal decomposition of **CI[1]**, **CI[2]**, **CI[3]**, **CI[4]** and **CI[5]** were occurred in three steps of weight loss (Baranwal, *et al.*, 2009). Yazdanbakhsh *et al.* (2009) proposed that the first stage of decomposition temperature corresponds to the removal of solvent molecules and some quantity interfering H_2O. The second stage the removal of coordinated H_2O, decomposition of acetic acid anions and reorganization of the complexes with the formation of metal-oxide as residue.

The complexes are prototypes of the general class of *basic carboxylates* where three metal ions form a triangle with an O atom at the centre to form a tri-oxo-nuclear complex. There are two carboxylate molecules bridging between the two metal ions (Anson *et al.*, 1997; Cotton, 1999). Three metals are attached with H_2O to form coordinated H_2O. From thermogram (**Figure 2.4**), basic process of decomposition is found to finish in the range of 250 – 290°C where solvated cluster and coordinated H_2O in the main cluster are eliminated. Water of hydration usually decomposes below 150°C and coordinated H_2O eliminated above 200°C. The decomposition of compound continues until the residue of complexes start to form.

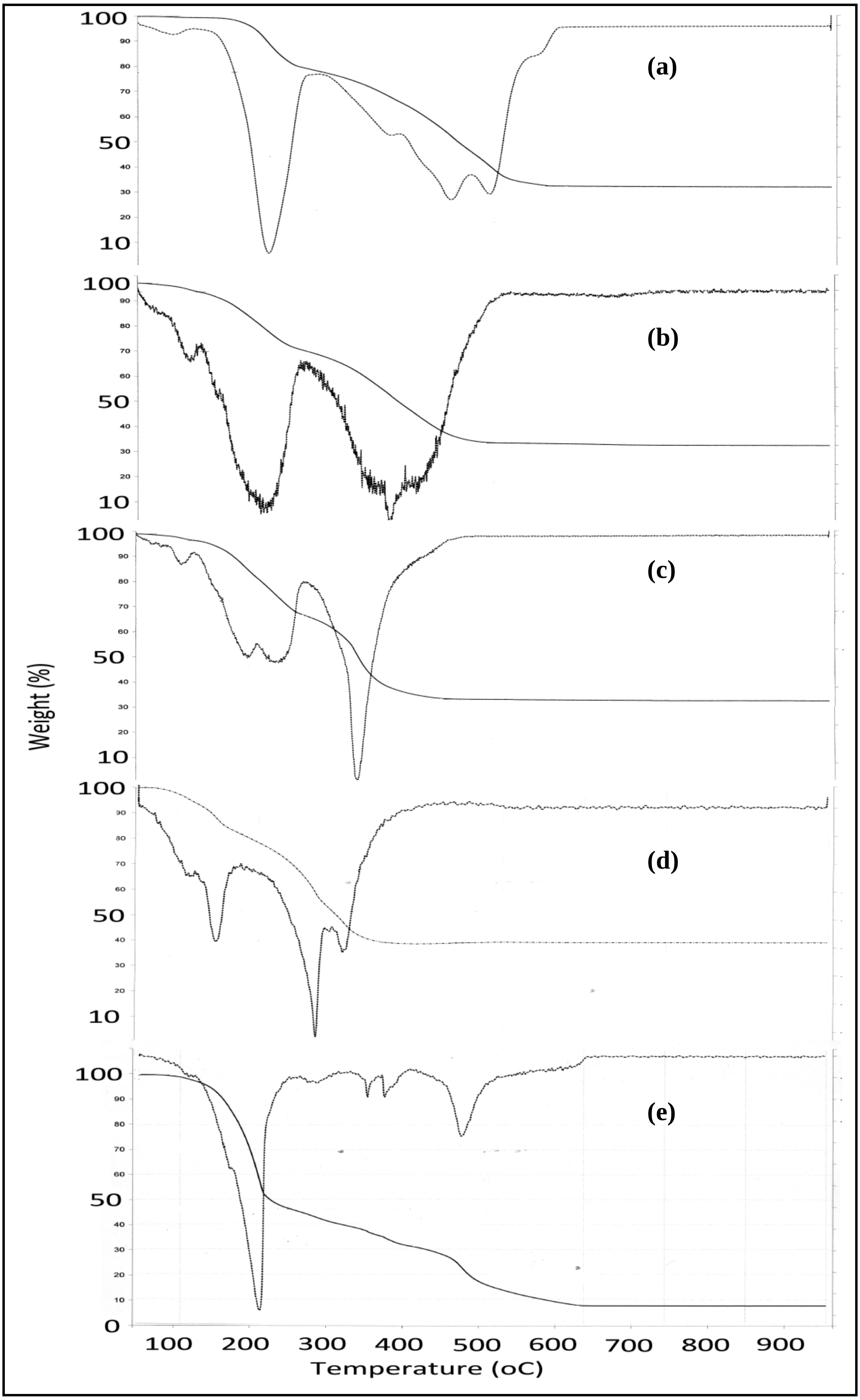

Figure 2.4: TGA thermogram of complexes: (a) Complex **CI[1]**, (b) Complex **CI[2]**, (c) Complex **CI[3]**, (d) Complex **CI[4]**, (e) Complex **CI[5]**

Table 2.8: Thermal analysis data of complexes

Complex	$T_{5\%}$ (°C)	Range of decomposition (°C)	Weight (%)	Residue compound
CI[1]	195	75 – 260	22	H_2O and CH_3COOH
		260 – 550	45	$[Cr_3O(CH_3COO)_6]^{4+}$
		550 above	32	Cr_2O_3
CI[2]	135	75 – 255	24	H_2O and CH_3COOH
		255 - 520	37	$[Cr_2FeO(CH_3COO)_6]^{4+}$
		520 above	36	Cr_2O_3, Fe_2O_3
CI[3]	160	75 – 260	30	H_2O and CH_3COOH
		260 – 460	33	$[CrFe_2O(CH_3COO)_6]^{4+}$
		460 above	34	Cr_2O_3, Fe_2O_3
CI[4]	120	75 – 180	18	H_2O and CH_3COOH
		180 – 460	42	$[Fe_3O(CH_3COO)_6]^{4+}$
		460 above	39	Fe_2O_3
CI[5]	150	75 – 250	53	H_2O and C_6H_5COOH
		250 - 610	39	$[Cr_3O(C_6H_5COO)_6]^{4+}$
		610 above	8	Cr_2O_3

Table 2.8 shows thermal analysis data for the complexes. **CI[1]** was found to have higher thermal stability compared to **CI[5]**. This suggests that ecetate groups have stronger bond than benzoate groups towards the Cr metal. Meanwhile, **CI[1]** is thermally more stable than **CI[4]**, this could possible due to electronic factors arising from the mixed spin in Fe. Sequence of thermal stability from the higher to the lower is **CI[1]** > **CI[3]** > **CI[5]** > **CI[2]** > **CI[4]**.

Based on TGA data and literature (Asamaki, *et al.*, 1995; Badea *et al.*, 2005; Baranwal, *et al.*, 2009; Grotowska, *et al.*, 1990) the proposed decomposition process of the complexes can be represented as the equation below:-

Temperature below 250^{o}C:

$[M_3O\ (RCOO)_6.3H_2O]NO_3.RCOOH \rightarrow [M_3O\ (RCOO)_6]^{4+}$ + gaseous product

Temperature below 500^{o}C:

$[M_3O\ (RCOO)_6]^{4+} \rightarrow M_2O_3$ (residue) + $RCOO^-$ (g)

Where, M = Cr(III), Fe(III) and R = CH_3, C_6H_5

2.3.6 X-ray crystallography

The structures of the complxes contain a triangular arrangement of metal ions connected by a central μ_3-oxo atom and bridged with six carboxylate ligands. Each carboxylate anion spans two metal centres at the periphery of the $[M_3(\mu_3\text{-}O)]^{6+}$ core, while the neutral monodentate ligands occupy the remaining coordination sites on each metal centre, and as a result the coordination around the metal centre is approximately octahedral (Yazdanbakhsh, *et al.*, 2009). Five complexes were synthesized namely **CI[1]**, **CI[2]**, **CI[3]**, **CI[4]** and **CI[5]**. However, only **CI[1]** and **CI[4]** were obtained in the crystalline form.

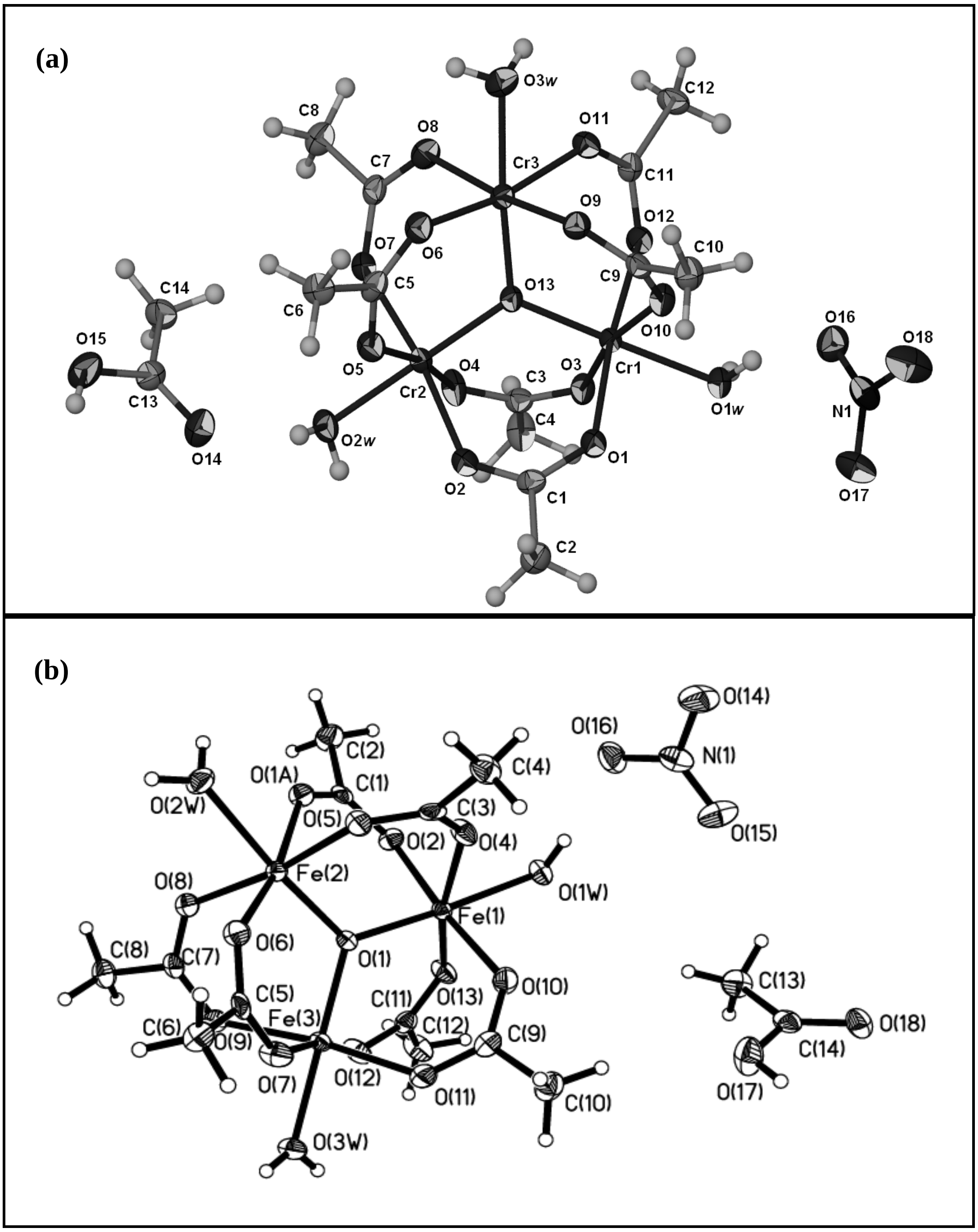

Figure 2.5: Thermal ellipsoid plot of (a) complex **CI[1]** (b) complex **CI[4]**

Table 2.9: Crystallographic data for **CI[1]** and **CI[4]**

Complex	**CI[1]**	**CI[4]**
Chemical formula	$[Cr_3(C_2H_3O_2)_6O(H_2O)_3]^+.$ $(NO_3)^-.C_2H_4O_2$	$[Fe_3(C_2H_3O_2)_6O(H_2O)_3]^+.$ $(NO_3)^-.C_2H_4O_2$
Formula weight	702.37	713.92
Crystal color	Green	Red
Temperature (K)	100 (2)	150
Crystal system	Monoclinic	Monoclinic
Space group	$P2_{1/c}$	$P2_1/c$
Crystal size (mm)	0.20 × 0.10 × 0.05	0.15 x 0.13 x 0.14
Unit cell dimensions:		
a (Å)	11.7034 (1)	11.7669 (5)
b (Å)	14.5102 (2)	14.5280 (6)
c (Å)	15.0427 (2)	15.1081 (6)
β (º)	91.532 (1)	91.835 (1)
Volume (Å^3)	2553.62 (5)	2581.40 (18)
Z	4	4
Density (Mgm^{-3})	1.827	1.837
Absorption coefficient, μ (mm^{-1})	1.35	1.76
F_{000}	1436	1460
θ range of data collection (º)	2.2–28.2	2.0 - 29.6
Limiting indices:		
h	−15→15	−16→15
k	−18→18	−19→18
l	−19→19	−20→20
R_{int}	0.046	0.040
Measured reflections	22819	14618
Independent reflections	5836	6740

a) CI[1]: $[Cr_3\text{-}O(C_2H_3O_2)_6(H_2O)_3]NO_3.CH_3CO_2H$

The green crystal of **CI[1]** has a monoclinic system with space group $P2_{1/c}$. The crystal data are shown in **Table 2.9**. Crystal structure of **CI[1]** is shown in **Figure 2.5a** as a thermal ellipsoid plot. The trinuclear $[Cr_3(CH_3CO_2)_6O\text{-}(H_2O)_3]$ cluster cation has an oxide atom that is connected to three water-coordinated Cr(III) atoms with the three Cr metal forming the points of an equilateral triangle. Each of the six acetate carboxylate groups bridge a Cr–O–Cr fragment.

CI[1] is a distorted octahedral with angles of O13—Cr1—O1W, O13—Cr2—O2W, O13—Cr3—O3W of 177.86°, 178.67° and 175.13° respectively. Meanwhile, angles for Cr1—O13—Cr2, Cr1—O13—Cr3, Cr2—O13—Cr3 were 119.96°, 119.74° and 120.30° respectively. Distance for Cr1—O13, Cr2—O13 and Cr3—O13 are 1.893 Å, 1.901 Å, 1.894 Å respectively (refer to Appendix **Tables A.1 – A.4**). The cluster cation interacts with the nitrate counter-ion and solvent molecules through O—H---O hydrogen bonds, forming a three-dimensional hydrogen-bonded network.

b) CI[4]: $[Fe_3\text{-}O(C_2H_3O_2)_6(H_2O)_3]NO_3.CH_3CO_2H$

CI[4] is a red crystal that has a monoclinic system and space group of $P2_1/n$. **Table 2.9** shows **CI[4]** crystal information and the structure is shown in **Figure 2.5b**. Three Fe(III) are connected with two acetate groups bridging reciprocally. Each Fe(III) is coordinated to H_2O and bonded to and O at the centre of the molecule. The cation cluster interacts with the nitrate counter-ion and solvent molecules through O—H---O hydrogen bonds, forming a three-dimensional hydrogen-bonded network (Yao, Liu, & Han, 2008).

The environment of all Fe(III) ions is a distorted octahedral geometry with angles of O1—Fe1—O1W, O1—Fe2—O2W, O1—Fe3—O3W of 176.64°, 173.01° and 177.84° respectively. Meanwhile, angles between Fe1—O1—Fe2, Fe2—O1—Fe3, Fe1—O1—Fe3 are 120.67°, 119.63° and 119.66°. Distance between Fe1—O1, Fe2—O1, Fe3—O1 a re 1.8982 Å, 1.8951 Å, 1.9124 Å respectively (refer to Appendix **Tables A.5 – A.8**) (Asamaki, *et al.*, 1995; François *et al.*, 2005).

2.3.7 Structure of complexes

The structures of **CI[1]**, **CI[2]**, **CI[3]**, **CI[4]** and **CI[5]**were proposed as shown in **Schemes 2.1, 2.2, 2.3, 2.4** and **2.5**. **CI[1]** and **CI[5]** contained three Cr^{3+} as metal nuclear while, **CI[4]** contained three Fe^{3+} as metal nuclear. **CI[2]** and **CI[3]** contained both metal nuclear ($Cr^{3+}$and Fe^{3+}) but in different ratios. **CI[2]** was built from two Cr^{3+}, one Fe^{3+} and **CI[3]** was built from one Cr^{3+}, two Fe^{3+}. **CI[1]**, **CI[2]**, **CI[3]** and **CI[4]** were made of acetate ligand while, **CI[5]** was made of benzoate ligand.

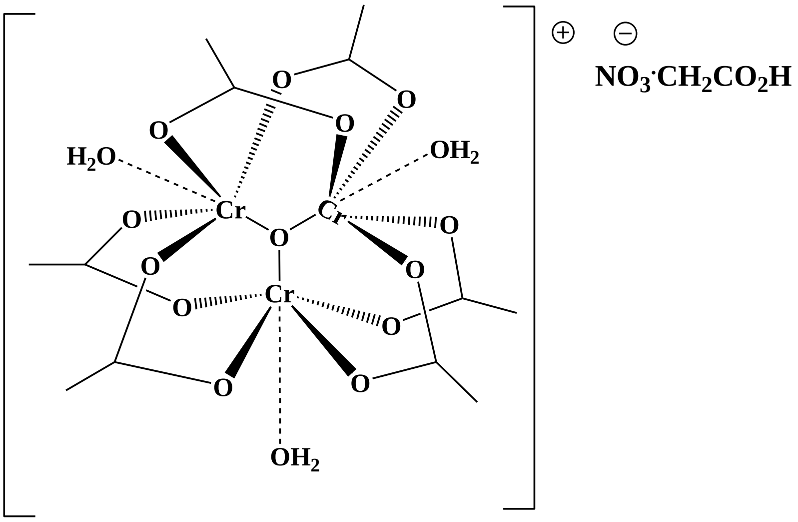

Scheme 2.1: Structure of **CI[1]**

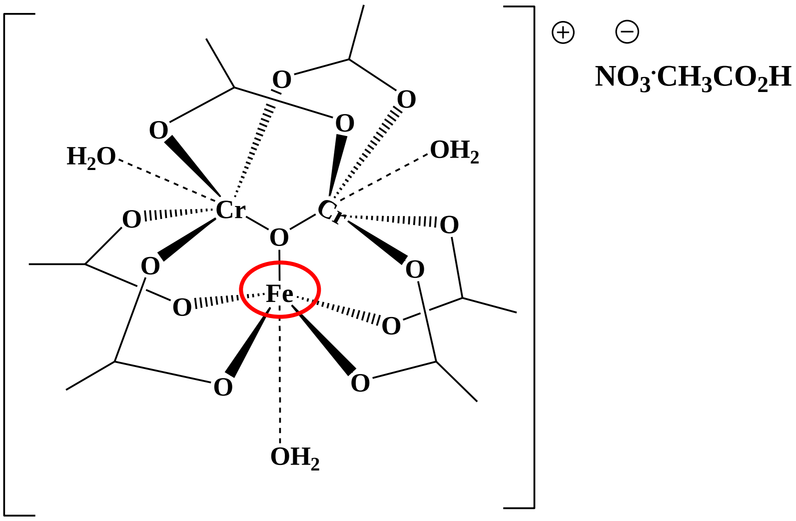

Scheme 2.2: Structure of **CI[2]**

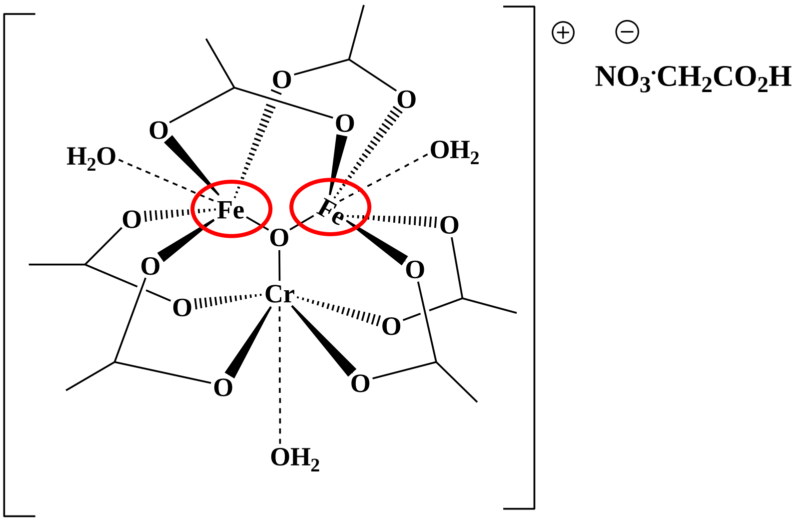

Scheme 2.3: Structure of **CI[3]**

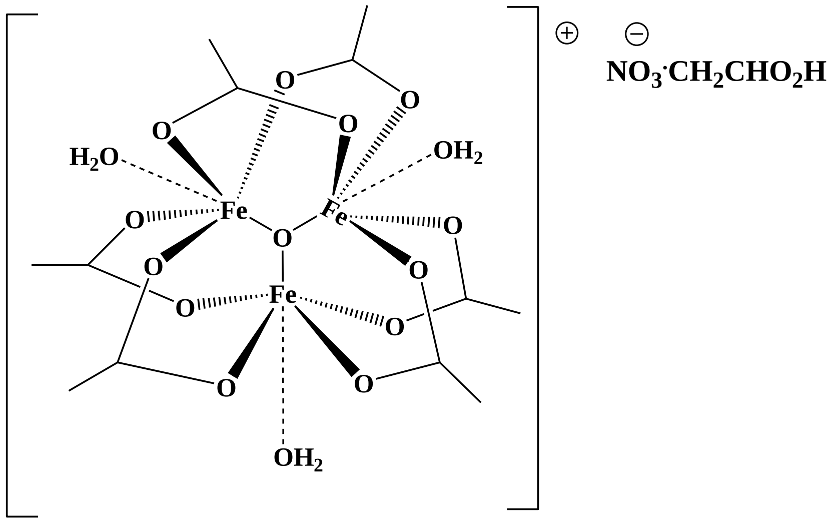

Scheme 2.4: Structure of **CI[4]**

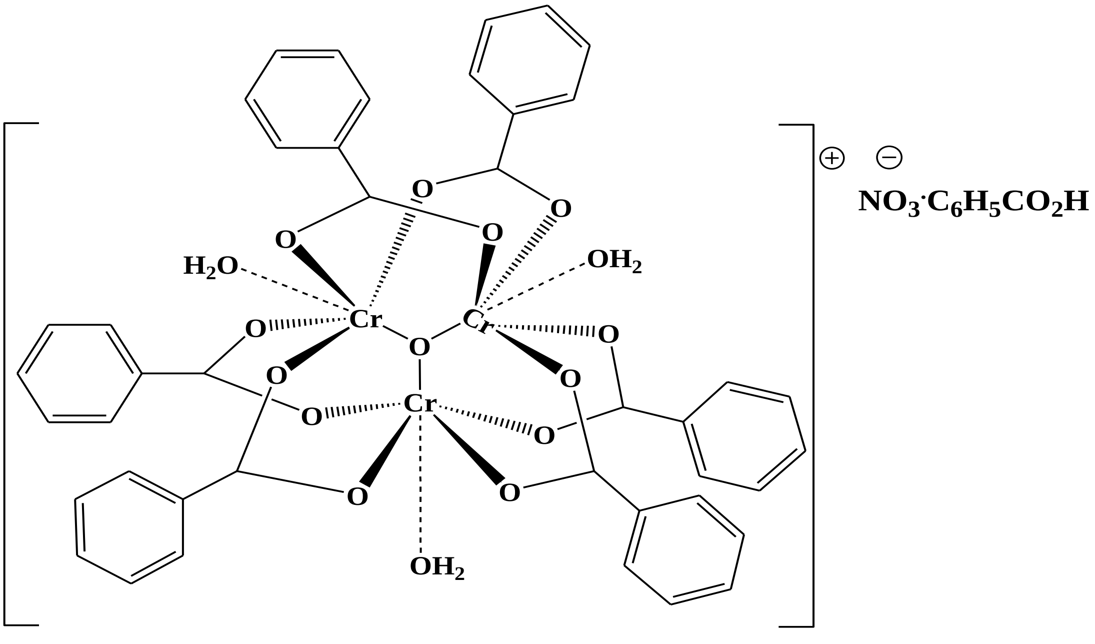

Scheme 2.5: Structure of **CI[5]**

References

Anson, C. E., Bourke, J. P., Cannon, R. D., Jayasooriya, U. A., Molinier, M., & Powell, A. K., (1997). Crystal Structures of the Isomorphous Prototypic Oxo-Centered Trinuclear Complexes $[Cr_3O(OOCCH_3)_6(H_2O)_3]Cl\cdot6H_2O$ and $[Fe_3O(OOCCH_3)_6(H2O)_3]Cl\cdot6H_2O$. *Inorganic Chemistry, 36*(6), 1265–1267.

Asamaki, K., Nakamoto, T., Kawata, S., Sano, H., Katada, M., & Endo, K. (1995). Structure and mixed-valence states of the trinuclear iron(II,III,III) pivalate complex-pivalic acid adduct, $[Fe_3O(O_2CCMe_3)_6(Me_3CCO_2H)_3]$ (Me = $-CH_3$). *Inorganica Chimica Acta, 236*(1–2), 155-161.

Badea, M., Olar, R., Vasile, G., Emandi, A., Pop, V., & Marinescu, D. (2005). Thermal behavior of some new chromium complexes with potential biological importance. *Journal of Thermal Analysis and Calorimetry, 81*(2), 273-276.

Baranwal, B. P., Das, S. S., Gupta, T., & Singh, A. K. (2002). Novel trinuclear, oxo-bridged materials of mixed-valence iron with fatty acids. *Progress in Crystal Growth and Characterization of Materials, 45*(1-2), 147-153.

Baranwal, B. P., & Fatma, T. (2005). Synthesis and characterization of oxo-bridged, trinuclear, six-coordinate mixed-carboxylato complexes of chromium(III). *Journal of Molecular Structure, 750*(1-3), 72-77.

Baranwal, B. P., Fatma, T., & Varma, A. (2009). Synthesis, spectral and thermal characterization of nano-sized, oxo-centered, trinuclear carboxylate-bridged chromium(III) complexes of hydroxycarboxylic acids. *Journal of Molecular Structure, 920*(1-3), 472-477.

Beatrice, M. D. S. B. (2009). *Synthesis of chromium(III) carboxylate complexes and their use in ziegler-natta polymerization.* Unpublished M.Sc. dissertation, University of Malaya, Kuala Lumpur.

Bond, A. M., Clark, R. J. H., Humphrey, D. G., Panayiotopoulos, P., Skelton, B. W., & White, A. H. (1998). Synthesis, characterisation and electrochemical reductions of oxo-centred, carboxylate-bridged triiron complexes. *Journal of the Chemical Society - Dalton Transactions*(11), 1845-1852.

Borawska, M. H., Koczoń, P., Piekut, J., Świsłocka, R., & Lewandowski, W. (2009). Vibrational spectra and antimicrobial activity of selected bivalent cation benzoates. *Journal of Molecular Structure, 919*(1–3), 284-289.

Coates, J. (2000). Interpretation of Infrared Spectra, A Practical Approach. In R. A. Meyers (Ed.), *Encyclopedia of Analytical Chemistry* (pp. 10815–10837). Chichester: John Wiley & Sons Ltd.

Cotton, F. A. (1999). *Advanced inorganic chemistry* (6 ed.). New York: John Wiley & Sons.

Dubicki, L., & Day, P. (1972). The electronic spectrum of trinuclear chromium(III) acetate. *Inorganic Chemistry, 11*(8), 1868-1875.

Fernandes, C., Stadler, E., Drago, V., da Cunha, C. J., & Kuwabara, I. H. (1996). Mössbauer, vibrational and electronic spectroscopy of trinuclear μ-oxo iron(III) acetate clusters with pyridine and derivatives as ligands. *Spectrochimica Acta Part A: Molecular and Biomolecular Spectroscopy, 52*(14), 1815-1821.

François, M., Saleh, M. I., Rabu, P., Souhassou, M., Malaman, B., & Steinmetz, J. (2005). Structural transition at 225 K of the trinuclear Fe(III) heptanoate [Fe3O(O2CC6H13)6(H2O)3]NO3. *Solid State Sciences, 7*(10), 1236-1246.

Gan, S. N., Aishah, M. J., & Ooi, C. P. (2000). Trinuclear oxo-centered chromium(III) carboxylate complexes as Ziegler-Natta catalysts for ethylene polymerization. In T. Sano, Uozumi, T., Nakatani, H and Terano, M. (Ed.), *Progress and Development of Catalytic Olefin Polymerization* (pp. 25-32). Tokyo: Technology and Education Publishers.

Gan, S. N., Lim, M. C., Chen, S. I., & Soga, K. (1987). Modified chromium(III) acetate used in the polymerization of α-olefins. *Journal of Catalyst, 105*, 249-253.

Glowiak, T., Kozlowski, H., Strinna Erre, L., & Micera, G. (1996). Crystal structure of μ3-oxo-esakis(μ2-acetate) triaquatrichromium(III) 2,6-dihydroxybenzoate dihydrate. *Inorganica Chimica Acta, 248*(1), 99-102.

Grotowska, M., Wojciechowska, R., & Wojciechowski, W. (1990). The thermal decomposition of some Cr(III) complexes. *Journal of Thermal Analysis, 36*(7-8), 2365-2373.

Lawrence, M. A., Maragh, P. T., & Dasgupta, T. P. (2012). Mechanistic studies of the selective reduction of ruthenium (III) containing trinuclear oxo complexes by l-ascorbic acid in aqueous solution. *Transition Metal Chemistry, 37*(6), 505-517.

Lawrence, M. A. W., Thomas, S. E., Maragh, P. T., & Dasgupta, T. P. (2011). Mechanistic studies on the intramolecular electron transfer in an adduct species of the oxo-centred trinuclear iron(III) cation and l-ascorbic acid in aqueous solution. *Transition Metal Chemistry, 36*(5), 553-563.

Losada, G., Mendiola, M. A., & Sevilla, M. T. (1997). Synthesis, characterization and electrochemical properties of trinuclear iron(III) complexes containing unsaturated carboxylate bridging ligands. *Inorganica Chimica Acta, 255*(1), 125-131.

Nakamoto, T., Hanaya, M., Katada, M., Endo, K., Kitagawa, S., & Sano, H. (1997). The Valence-Detrapping Phase Transition in a Crystal of the Mixed-Valence Trinuclear Iron Cyanoacetate Complex $[Fe_3O(O_2CCH_2CN)_6(H_2O)_3]$. *Inorganic Chemistry, 36*(20), 4347-4359.

Nakamoto, T., Katada, M., & Sano, H. (1999). Mixed-valence states of iron long-chain carboxylate complexes. *Inorganica Chimica Acta, 291*(1–2), 127-135.

Ooi, C. P. (1996). *The use of trinuclear chromium(III) complexes as Ziegler-Natta catalysts for the polymerization of ethylene*. Unpublished M.Sc. dissertation, University of Malaya, Kuala Lumpur.

Schatschneider, B., & Perumareddi, J. R. (2005). UV–Vis absorption study of some tetragonal chromium(III) complexes. *Inorganica Chimica Acta, 358*(15), 4571-4574.

Tan, S. H. (2007). *Synthesis of chromium(III) acetate and chloroacetate complexes and their application in olefin polymerization.* M.Sc. dissertation, University of Malaya, Kuala Lumpur.

Wong, J. X. (2010). *Synthesis of chromium-based Ziegler-Natta catalysts and thier application in ethylene polymerization and copolymerization.* M.Sc. dissertation, University of Malaya, Kuala Lumpur.

Wu, R., Jayasooriya, U. A., & Cannon, R. D. (2000). Vibrational coupling in oxo-centred trinuclear clusters: oxygen-16/18 isotopic substitution studies of $[FeIII_3O(O_2CC(CH_3)_3)_6(py)_3][FeCl_4]$ and $[FeIII_2FeIIO(O_2CC(CH_3)_3)_6(py)_3]$. *Spectrochimica Acta Part A: Molecular and Biomolecular Spectroscopy, 56*(3), 575-579.

Wu, R., Poyraz, M., Sowrey, F. E., Anson, C. E., Wocadlo, S., Powell, A. K., *et al.* (1998). Electron Localization and Delocalization in Mixed-Valence Transition Metal Clusters: Structural and Spectroscopic Studies of Oxo-Centered Trinuclear Complexes $[Fe_3O(OOCCMe_3)_6(py)_3]^{+/0}$ and $[Mn_3O(OOCCMe_3)_6(py)_3]^{+/0}$. *Inorganic Chemistry, 37*(8), 1913-1921.

Yao, S., Liu, J., & Han, Q. (2008). Hexa-[mu]2-acetato-triaqua-[mu]3-oxido-triiron(III) nitrate acetic acid solvate. *Acta Crystallographica Section E, 64*(8), m989.

Yazdanbakhsh, M., Lotfian, N., & Tavakkoli, H. (2009). Synthesis and characterization of two novel trinuclear oxo-centered, of chromium and iron complexes containing unsaturated carboxylate bridging ligand. *Bulletin of the Chemical Society of Ethiopia, 23*(3), 463-466.

Yazdanbakhsh, M., Tavakkoli, H., Taherzadeh, M., & Boese, R. (2010). Synthesis, X-ray crystal structure and spectroscopic characterization of heterotrinuclear oxo-centered complex $[Fe_2NiO(CH_3CH_2COO)_6(H_2O)_3]$. *Journal of Molecular Structure, 982*(1-3), 176-180.